Asian Journal of Chemistry; Vol. 27, No. 5 (2015), 1635-1640

ASIAN JOURNAL OF CHEMISTRY

http://dx.doi.org/10.14233/ajchem.2015.17397

Condensed Phase Species Composition for Aluminum Particles Combustion in Nitrocellulose

H.B. PEI*, J.X. NIE and Q.J. JIAO

State Key Laboratory of Explosion Science and Technology, Beijing Institute of Technology, Beijing 100081, P.R. China

*Corresponding author: Tel./Fax: +86 10 68914863; Email: hongbo2751@sina.com

Received: 14 February 2014; *Accepted*: 6 May 2014; *Published online*: 20 February 2015; AJC-16858

The mixtures of nitrocellulose and aluminum with different particle size were ignited in a hermetic steel chamber. The pressures of combustion products were measured and the condensed products were recovered. The morphology and surface atomic distribution of the condensed products was studied with scanning electron microscopy and energy dispersive spectroscopy. The crystal structure and composition of condensed products were analyzed by X-ray diffraction. The results show that the products particles are still spherical shape whose size is roughly identical to that of the initial particles for micro aluminum particles. An analysis of condensed products morphology indicates that the reaction of aluminum proceeds on the particle surface. The amount of reacted aluminum importantly depends on the particles size of aluminum. Non-reacted aluminum, Al_2O_3 and Al_2OC were founded in condensed products. γ-Al_2O_3 is present in all samples and α-Al_2O_3 is found only in the sample containing nano Al. The mass fraction of Al_2OC varied ranged from 2 to 27 % with the Al particles size changed in condensed products.

Keywords: Combustion product, Morphology, Propellant, Al_2OC.

INTRODUCTION

Aluminum is widely used as a fuel additive in propellants and explosives to improving their energy characteristics. Aluminum typically reacts with the combustion or detonation products of the energetic oxidizer and binder, such as CO_2, CO and H_2O, when aluminum burns in a composite solid propellant. For this reason, the properties of aluminum burning, such as ignition temperature, ignition delay time, burn time, burning rate and flame speed, in various oxidizer environments have been intensively studied[1-9]. However, much less attention was given to the condensed combustion products of aluminum in propellant. It usually thought the products of aluminum reacting with the decomposition of propellant is Al_2O_3. However, researches have shown that Al_2OC, Al_4C_3, Al_4O_4C may produce when the oxidizer containing carbon[10-14] and AlN may produce at N_2 containing atmosphere[15-18].

The formation of condensed combustion products is very important to understand the physical and chemical picture of combustion. They can also enrich our understanding of the energy output or combustion mechanicals of mixtures contain aluminum.

Nitrocellulose is widely used in single or double base propellant. In this study, aluminum was incorporated to nitrocellulose, the mixtures were initiated by igniter in a steel chamber and the condensed product is recovered. So, it would easily to analyze the condensed product when aluminum is incorporated.

The morphology and surface atomic distribution of the condensed products was studied with scanning electron microscopy and energy dispersive spectroscopy on HITACHI S4700. The crystal structure and composition of powders were analyzed by X-ray diffraction on a Philips X'pert MRD X-ray diffractometer using unfiltered CuK_α radiation. The phases and quantitative phase composition of condensed products were determined by the computer program MDI Jade 6.5.

EXPERIMENTAL

One type of nano aluminum particle and four types of micro aluminum particle were used in this study. Representative electron microscope images of the particles are shown in Fig. 1. Five fine particles have nearly ideal spherical particles. Nano Al: median diameter is about 50 nm; the pure aluminum content is 76 %. Micro Al: median diameter 2 μm (98.1 % Al), 10 μm (98.6 % Al), 30 μm (99 % Al), 90 μm (99.5 % Al), the particle sizes were analyzed using analyzed using laser particle sizer (Mastersizer2000). Nitrocellulose used in the experiment contains 12 % nitrogen by weight, whose molecular formula is $C_{22.74}H_{29.33}O_{36.08}N_{8.57}$ and the standard enthalpy of formation is kJ/kg.

Mixtures: The combustion of nitrocellulose and aluminum were carried out in a hermetic steel chamber with an internal volume of about 0.5 L. The outer diameter of the chamber is 80 mm and it can hold the gas pressure in the range of vacuum

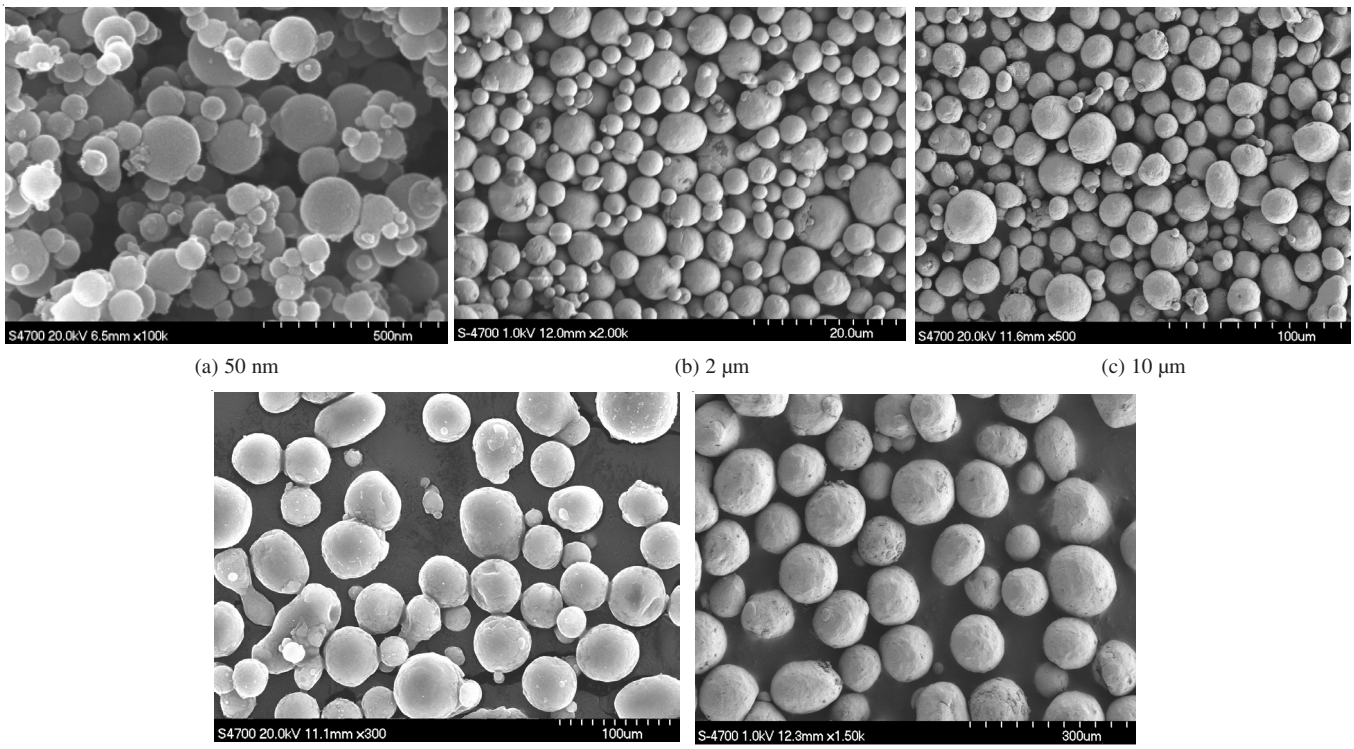

(a) 50 nm (b) 2 μm (c) 10 μm

(d) 30 μm (e) 90 μm

Fig.1. SEM images of the Al particle used in experiment

to 20 MPa. The mixtures are shown in Table-1. According the amount of oxygen, 1 kg nitrocellulose can reacts with 0.65 kg aluminum at most theoretically corresponding to the aluminum content of 39.3 %. The mass of sample containing aluminum particles is 2.25 g and the content of aluminum is 20 % by weight. The aluminum can be oxidized completely theoretically. The calculated peak pressure of combustion product is around 5 MPa in the hermetic steel chamber if all aluminum reacted completely.

TABLE-1
MIXTURES OF COMBUSTION

Sample No.	Formulae	Particle size (μm)	Density (g/cm^3)
N1	NC (1.8 g)	NA	0.60
N2	NC (1.8 g) + Al_2O_3 (0.45 g)	NA	0.64
N3	NC (1.8 g) + Al (0.45 g)	90	0.63
N4	NC (1.8 g) + Al (0.45 g)	30	0.63
N5	NC (1.8 g) + Al (0.45 g)	10	0.63
N6	NC (1.8 g) + Al (0.45 g)	2	0.62
N7	NC (1.8 g) + Al (0.45 g)	0.05	0.52

NC = Nitrocellulose; Al = Aluminium

Pressure testing apparatus: The reaction heat will be increased markedly if aluminum reacted with decomposition of nitrocellulose and the products overpressure would be increased too. The more the aluminum reacts, the higher the overpressure is. So pressure test was used to evaluate the reaction of aluminum. The schematic of pressure testing apparatus is shown in Fig. 2, which mainly contain piezoresistive pressure sensor, digital recorder and a computer. The pressure sensor is CY-400 with the pressure range of 0-10 MPa, the response frequency > 100 KHz and the measuring error of ± 3 %. The pressure sensor was mounted in the wall of chamber with screw thread. The digital recorder is TST6150 with the maximal sampling frequency of 20 MHz/channel.

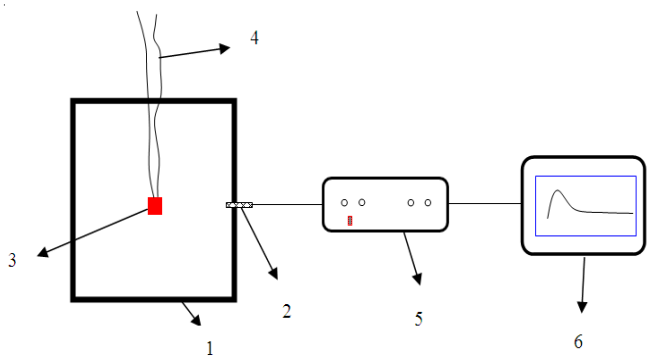

Fig. 2. Schematic diagram of the pressure testing apparatus: (1) Hermetic steel chamber, (2) pressure sensor, (3) mixture sample, (4) igniter leads, (5) digital recorder, (6) computer

In the experiment, the mixture and igniter were placed in a furnace with a 20 mm diameter and 20 mm height. The mixture is pressed with a glass stick. Their density is shown in Table-1. The furnace was placed in the center of the chamber. After the chamber was closed, the igniter was initiated. At the same time, the digital recorder is triggered and begins to detect the pressure of combustion products. The condensed residues after combustion in the chamber were recovered and analyzed to determine their composition. In each case, the residue recovered from the chamber was first sieved (to remove fragments of igniter and its electric leads) and then dried for 2 h at 100 °C.

RESULTS AND DISCUSSION

Peak overpressure of combustion products: A representative overpressure of combustion products is showed in Fig. 3. The pressure fluctuated widely because the reflection of shock in the pressure sensor. The smooth line was obtained by average eight points through the data. Three tests were carried out of each mixture to get the average peak overpressures. The average peak overpressures of varies mixtures are presented in Table-2.

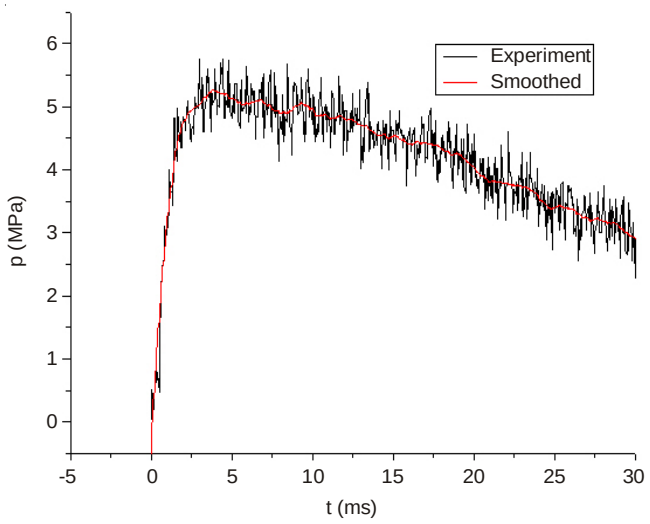

Fig. 3. Overpressure profile of combustion products for N1

Al_2O_3 as an inert additive was used to compare with other mixtures, because it has similar thermal capacity to aluminum. Table-3 showed the introduction of Al_2O_3 would decrease peak over pressure due to absorbing heat of Al_2O_3. The peak overpressure of N3 sample is higher than pure nitrocellulose, which indicates that aluminum has reacted with the decomposition of nitrocellulose. With the particles size of aluminum decreased, the peak overpressure increases. The peak overpressure of N3 (90 μm aluminum) is similar to that of pure nitrocellulose. But consider that the non-reacted aluminum will absorb some heat from the gas combustion as Al_2O_3, the content of reacted aluminum is still considerable. The peak overpressure of N7 (50 nm aluminum) increased 29.8 % compared with pure nitrocellulose. The results shows that the fraction of reacted aluminum increases when the particle size of aluminum decreases and the amount of reacted aluminum importantly depended on the particles size of aluminum.

TABLE-2
PEAK OVERPRESSURE (p_k) OF COMBUSTION PRODUCTS

Sample No.	Particle size (μm)	p_k (MPa)
N1	NA	5.12
N2	NA	4.96
N3	90	5.15
N4	30	5.40
N5	10	5.46
N6	2	5.95
N7	0.05	6.65

Morphology of condensed combustion products: The condensed combustion product is grayer powder. The SEM images of condensed combustion products for different samples are shown in Fig. 4.

The typical combustion product of nano aluminum is shown in Fig. 4 (a), no sphere particle were found in nano aluminum combustion product. It appears that all particles have condensed together. Research has showed that nano aluminum

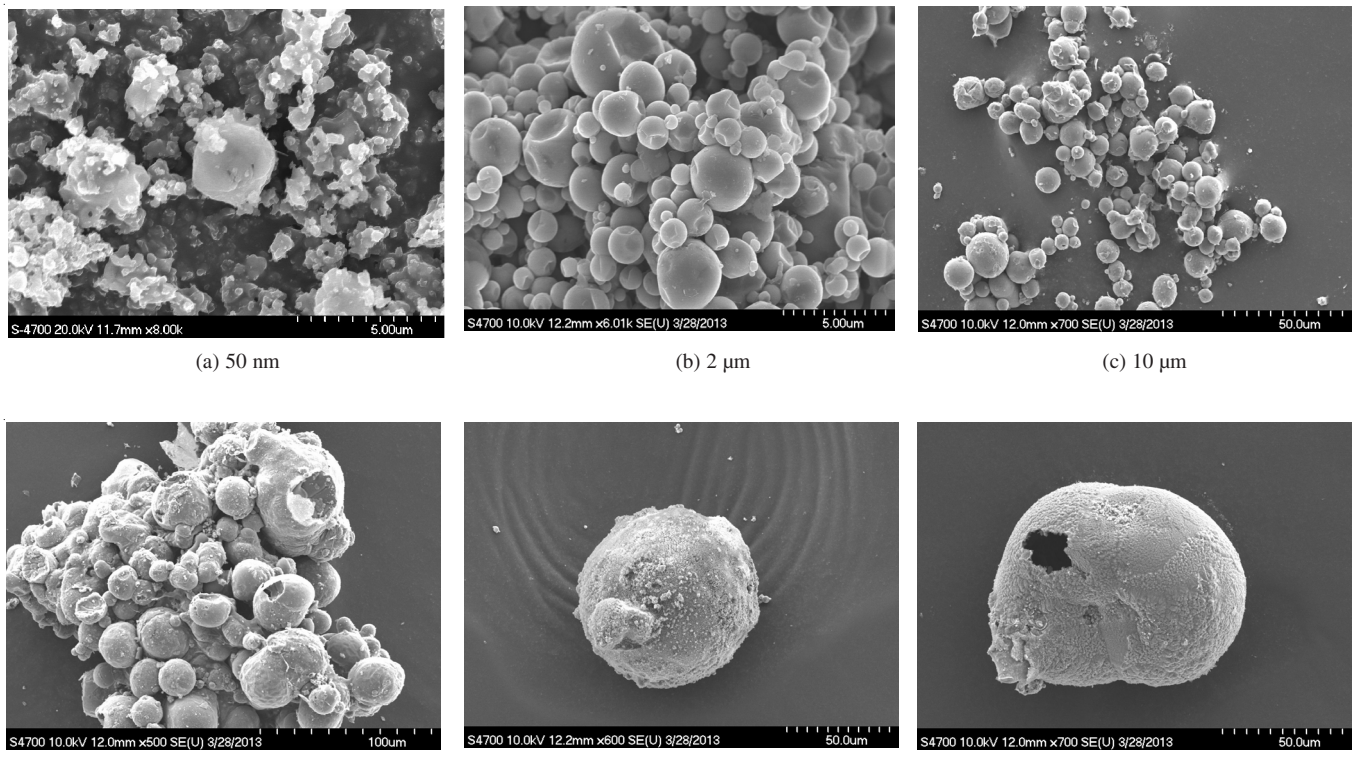

(a) 50 nm (b) 2 μm (c) 10 μm

(d) 30 μm (e) 90 μm (f) 90 μm

Fig. 4 SEM images of condensed combustion products

can ignited around 800 K in O_2 environment[19]. The flame temperature of nitrocellulose is around 2700 K, which is much higher than the ignition temperature of nano aluminum. So the nano aluminum particles should be ignition easily in this temperature. The reasonable explanation for producing products as present is because that the combustion products are molten in the flame of nitrocellulose and then these molten particles condensed together.

The combustion products of micro aluminum is obviously different from nano aluminum. In most tests, the particles are still spherical shape whose size is roughly identical to that of the initial particles. It is well known that metal particle combustion can occur in two essentially different regimes[3,20]. The first, heterogeneous combustion, occurs by metal oxidation on the metal particle surface and results in the size of the oxide particle formed during heterogeneous combustion being close to the initial size of the metal particle. The second regime, gas-phase combustion, proceeds by three sequential steps; (1) metal vaporization; (2) oxidation of the metal vapor with the formation of intermediate gaseous products of combustion; (3) condensation of the gaseous oxide with formation of ultrafine oxide particles. Unlike the first regime, the size of the oxide particles formed during the gas-phase combustion does not depend significantly on the initial metal particle size and only depends weakly on the type of burning metal. For Al, the oxide particle size of gas-phase combustion is about 0.03-0.1 μm[20]. In our experiment, the products particle is closed to the initiation particles. This correlates with the theories of aluminum oxidation on the surface of a burning drop[21].

Hollow particles were found [Fig. 4(d) and (f)], which has also been found by other researchers[10,17,21-24]. The reason of hollow particles formed is possibility that the molten aluminum flow out of the oxide shell[22], which also indicates the reaction of aluminum particles is heterogeneous surface reaction. In Fig. 4(b), it can be see that most spherical particles surface has a depression and which also occurred on (c) and (d). The reason is the same that producing hollow particles. The distinguish is that the hole was sealing up and the hole can't be observe. But the center of these particles is still hollow.

Composition of condensed combustion products

Surface elemental composition: Energy dispersive spectroscopy (EDS) was employed for elemental composition analyses. A rectangle zone of the particle surface was chosen (Fig. 5). Quantitative results of the composition analyses are presented in Table-3. For all samples, only C, O and Al were found. Nitrogen was not detected in any of the sample, which implied there is no nitride formed. Considered the error of EDS, the elemental composition of different samples is similar. The elemental ratio of aluminum to oxygen is about 1:1.

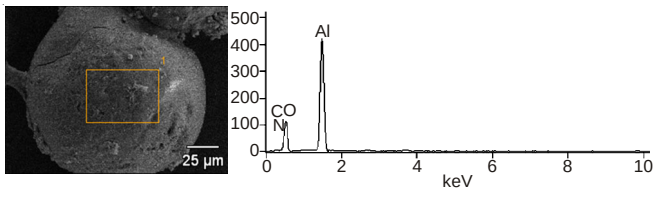

Fig. 5 (a) EDS zone, (b) EDS profile

TABLE-3
ELEMENTAL COMPOSITION OF
DIFFERENT CONDENSED PRODUCTS

Al particles size	Elemental compositions	C	O	Al
90 μm	Wt (%)	3.8	41.6	54.6
	At (%)	6.4	52.6	41.0
30 μm	Wt (%)	10.2	34.4	55.4
	At (%)	16.8	42.6	40.6
10 μm	Wt (%)	5.0	41.8	53.2
	At (%)	8.3	53.2	39.5
2 μm	Wt (%)	8.4	38.8	52.8
	At (%)	13.8	47.7	38.5
50 nm	Wt* (%)	7.3	35.3	57.4
	At (%)	12.4	44.6	43.1

Combustion products composition: Fig. 6 shows the XRD patterns of samples with different particles size Al. It is seen that the peak of XRD patter is similar, but the line intensities is different. Qualitative phase analysis identified the phase aluminum (PDF 04-0787), γ-Al_2O_3 (PDF 10-0425), α-Al_2O_3 (PDF 46-1212) and Al_2OC (PDF 36-0418). α-Al_2O_3 is found only in the sample containing nano aluminum.

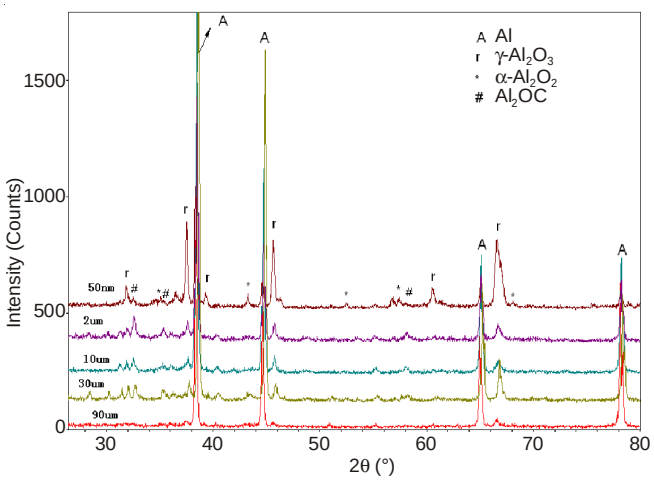

Fig. 6. XRD results of condensed combustion products

The composition fraction of the combustion products is determined by MDI Jade 6.5 program and the results are presented in Table-4.

TABLE-4
CRYSTAL PHASE COMPOSITIONS
OF CONDENSED PRODUCTS

Sample No.	Particle size	Al	Al_2O_3	Al_2O_3	Al_2OC
N3	90 μm	91 ± 5	7 ± 1	0	2 ± 1
N4	30 μm	82 ± 5	10 ± 2	0	8 ± 1
N5	10 μm	67 ± 4	23 ± 3	0	10 ± 2
N6	2 μm	38 ± 3	35 ± 3	0	27 ± 3
N7	50 nm	10 ± 2	76 ± 5	8 ± 1	6 ± 1

The results of the quantitative analysis showed that the mass fraction of aluminum decrease with the particle size decreased. The fraction of non-reacted aluminum is around 91 % for 90 μm aluminum particles, which indicates that a majority of aluminum didn't participate in the reaction. This result is consistent with the over pressure results. This is because

the combustion of aluminum with decomposition of nitrocellulose is surface oxidation. In the process of oxidation, the aluminum core is covered with the oxide shell which preventing the reaction. The transportation of reactant traverse the oxide shell is more difficult for bigger particles compared with small particles. So the amount of non-reacted aluminum rises when aluminum particles size increased. About 10 % non-reacted aluminum was found for 50 nm aluminum particles. This can be caused by two reasons. The first is that aluminum in the center didn't reacted because of the preventing of Al_2O_3 and the other is that aluminum particles agglomerated when preparing the samples. The mass fraction of Al_2OC and Al_2O_3 increased with the particle size decreased for micro aluminum. The mass fraction of Al_2O_3 in 50 nm samples is higher than that in micro aluminum samples, but the mass fraction of Al_2OC decreased compared with 2 and 10 μm samples.

Energy dispersive spectroscopy (EDS) shows that the elemental ratio of O to Al is around 1:1, which is lower than elemental ratio of O to Al in Al_2O_3. It is because there are Al_2OC formed according the XRD results. The element fraction of aluminum in 90 μm sample is higher than 90 % determined by XRD, but EDS shows element fraction is about 54 %. The difference is due to the detecting depth of EDS. Energy dispersive spectroscopy (EDS) can only detected the surface element of particles. So the fraction of aluminum determined by EDS is much higher than that determined by XRD. The elemental ratio of O to C in different samples determined by EDS and XRD is presented in Table-5. It shows that the elemental ratio of O to C determined by EDS is close to that determined by XRD except 50 nm aluminum particles. For 50 nm aluminum, the elemental faction of C determined by XRD is much lower than that determined by XRD. The reason is possible formation of amorphous carbon which can not be detected by XRD.

TABLE-5
ELEMENTAL RATIO OF O TO C

Particle size	50 nm	2 μm	10 μm	30 μm	90 μm
EDS	3.6	3.4	6.4	2.5	8.2
XRD	32.4	3.3	6.5	3.9	9.6

Assovskii *et al.*[11] studied the solid combustion products of aluminum in CO_2. Qualitative analysis shows that the condensed product contains Al_2OC, Various phases (α, γ, δ) of the oxide Al_2O_3 and a little non-reacted aluminum. Trunov *et al.*[25] studied the Al_2O_3 phase transformations in the temperature ranges from 300 to 1500 K. Usually, when the temperature increases to about 820-1300 K, γ-Al_2O_3 transforms into γ-Al_2O_3 and then transforms into thermodynamically stable α-Al_2O_3 at about 1400 K. The adiabatic flame temperature of nitrocellulose is about 2710 K, which is high enough to transform α-Al_2O_3 to α-Al_2O_3. However in this study, γ phase Al_2O_3 was found in sample containing nano aluminum. This can be explains as follows: the activation of γ-Al_2O_3 to α-Al_2O_3 is high, so the process of γ-Al_2O_3 to α-Al_2O_3 is slow, but the combustion of aluminum is very fast, α-Al_2O_3 has no time to form α-Al_2O_3.

Both the EDS and XRD analysis show there is no Al-N formed in the combustion product. Gromov *et al.*[18] has reported the content of Al-N in recovered products is over 50 % by weight at 2800 K for 100 nm aluminum burning in air. Previous workers have studied[15] the combustion nano-Al/RDX in O_2 and Ar in a shock wave tube. Al-N was found only in Ar atmosphere. The products of nitrocellulose determined by thermodynamic equilibrium program REAL is presented in Table-6. In the decomposition of nitrocellulose, there contain about 12 % N_2 by weight. The difference can be explained that the content of N_2 in the gas products is small compared with air; also the reaction of aluminum with H_2O or oxycarbide is more easily compared with N_2.

TABLE-6
MASS FRACTION OF DECOMPOSITION
OF NC (v = 0.27 m^3/kg, ΔU = 0 kJ/kg)

Species	CO	CO_2	H_2O	N_2	H_2
Mass fraction (%)	52 %	19 %	17 %	12 %	1 %

There have two possible pathways to form Al_2OC. The first is that aluminum reacts with C or CO to form Al_3C_4, then Al_3C_4 reacts with Al_2O_3 to form Al_2OC[13]. The other pathway is that CO reacts directly with molten aluminum producing Al_2OC[11]. The first pathway is the condensed reaction and the reaction rate is slow, so it takes a long time (about several 10 min) to form considerable amounts of Al_2OC[13]. In our experiment the reaction is very fast, if the reaction pathway was the first, Al_3C_4 should be detected too. The second pathway is the reaction of condensed matter with gas and the reaction rate is much faster than that in the first. Also it contains large amount of CO in the decomposition of nitrocellulose as presented in Table-6. So it can be concluded that the most reasonable pathway to form Al_2OC is second.

The major reaction between aluminum and decomposition of nitrocellulose producing Al_2O_3 are:

$$2Al + 3CO_2 \rightarrow Al_2O_3 + 3CO, \text{-826 kJ/mol} \quad (1)$$

$$2Al + 3H_2O\ (gas) \rightarrow Al_2O_3 + 3H_2, \text{-949 kJ/mol} \quad (2)$$

$$2Al + 3CO \rightarrow Al_2O_3 + 3C, \text{-1345 kJ/mol} \quad (3)$$

The reaction of Al with CO producing Al_2OC (Δ_fH_m = -720.3 kJ/mol[12]) is:

$$2Al + CO \rightarrow Al_2OC, \text{-610 kJ/mol} \quad (4)$$

According to the eqn. 4, the formation of Al_2OC would decrease the reaction heat compared with formation of Al_2O_3 when aluminum reacts with decomposition of nitrocellulose. Also it would markedly decrease the mass of gas. Both of these would reduce the specific impulse of propellant, which should be considered when evaluate the performance of propellant containing aluminum particles.

Conclusion

The combustion of aluminum with different particle size in the decomposition of nitrocellulose was studied. The condensed combustion product is grayer powder. SEM results shows that the product particles for micro aluminum are still spherical shape whose size is roughly identical to that of the initial particles. An analysis of condensed products morphology indicates that the reaction of aluminum proceeds on the particle surface. Both pressure measured results and XRD results shows that the amount of reacted aluminum importantly depended on the particles size of aluminum. The condensed products of aluminum reacting with the decomposition of nitrocellulose are Al_2O_3 and Al_2OC. No nitride was found in

the condensed products. γ-Al_2O_3 is present in all samples and α-Al_2O_3 is found only in the sample containing nano aluminum. A reasonable explanation the formation of Al_2OC is that molten aluminum reacts with CO.

REFERENCES

1. S.E. Olsen and M.W. Beckstead, *J. Propul. Power*, **12**, 662 (1996).
2. E.L. Dreizin, *Pror. Energy Combust. Sci*., **26**, 57 (2000).
3. T. Bazyn, H. Krier and N. Glumac, *Proc. Combust. Inst*., **31**, 2021 (2007).
4. R.A. Yetter, G.A. Risha and S.F. Son, *Proc. Combust. Inst*., **32**, 1819 (2009).
5. M.W. Beckstead, *Combust. Explos*., **41**, 533 (2005).
6. P. Bucher, R.A. Yetter, F.L. Dryer, T.P. Parr, D.M. Hanson-Parr and E.P. Viceni, *Proc. Combust. Inst*., **26**, 1899 (1996).
7. P. Bucher, R.A. Yetter, F.L. Dryer, T.P. Parr and D.M. Hanson-Parr, *Proc. Combust. Inst.*, **27**, 2421 (1998).
8. M.A. Trunov, M. Schoenitz and E.L. Dreizin, *Propellants Explos. Pyrotech*., **30**, 36 (2005).
9. A.V. Fedorov and Y.V. Kharlamova, *Combust. Explos*., **39**, 544 (2003).
10. K. Brandstadt, D.L. Frost and J.A. Kozinski, *Proc. Combust. Inst*., **32**, 1913 (2009).
11. I.G. Assovskii, A.N. Streletskii and V.I. Kolesnikov-Svinarev, *Dokl. Phys. Chem*., **405**, 235 (2005).
12. S. Rossi, E. Dreizin and C.K. Law, *Combust. Sci. Technol*., **164**, 209 (2001).
13. J.M. Lihrmann, T. Zambetakis and M. Daire, *J. Am. Ceram. Soc*., **72**, 1704 (1989).
14. V. Sarou-kanian, J.C. Rifflet, F. Millot, E. Veron, T. Sauvage and I. Gökalp, *Combust. Sci. Technol*., **177**, 2299 (2005).
15. M. Najjari, H. Mnif, H. Samet and N. Masmoudi, *J. Phys. D Appl. Phys*., **41**, 1 (2008).
16. W. Trzcinski, S. Cudzilo and L. Szymanczyk, *Propellants Explos. Pyrotech*, **32**, 392 (2007).
17. P. Bucher, R.A. Yetter, E.L. Dryer, E. Vicenzi, T. Parr and D. Hansonparr, *Combust. Flame*, **117**, 351 (1999).
18. A. Gromov and V. Vereshchagin, *J. Eur. Ceram. Soc*., **24**, 2879 (2004).
19. H.B. Pei, Y. Liu and H. Ren, *Adv. Mater. Res., 771*, 113 (2013).
20. I.S. Altman, *Combust. Sci. Technol*., **160**, 221 (2000).
21. S.D. Gilev and V.F. Anisichkin, *Combust. Explos*., **42**, 107 (2006).
22. J.E. Crump, J.L. Prentice and K.J. Kraeutle, *Combust. Sci. Technol*., **1**, 205 (1969).
23. R. Friedman and A. Macek, *Combust. Flame*, **6**, 9 (1962).
24. A. Davis, *Combust. Flame*, **7**, 359 (1963).
25. M.A. Trunov, M. Schoenitz, X. Zhu and E.L. Dreizin, *Combust. Flame*, **140**, 310 (2005).